Supporting Information

Synthesis, Structural Elucidation and Diffusion-Ordered NMR studies of Homoleptic Alkyl Lithium Magnesiates: Donor-Controlled Structural Variations in Mixed-Metal Chemistry

Sharon E. Baillie,[†] William Clegg,[‡] Pablo García-Álvarez,[§] Eva Hevia,*[†] Alan R. Kennedy,[†] Jan Klett[†] and Luca Russo[‡]

[†] *WestCHEM, Department of Pure and Applied Chemistry, University of Strathclyde, Glasgow, UK, G1 1XL*
[‡] *School of Chemistry, Newcastle University, Newcastle upon Tyne, UK, NE1 7RU*
[§] *Departamento de Química Orgánica e Inorgánica-IUQOEM, Universidad de Oviedo-CSIC, E-33071 Oviedo, Spain*

Table S1: Key crystallographic and refinement parameters for compounds 2–7

	2	**3**	**4**	**5**	**6**	**7**
Empirical formula	$C_{16}H_{40}LiMgOSi_3$	$C_{20}H_{49}LiMgO_4Si_3$	$C_{14}H_{37}LiMgOSi_3$	$C_{28}H_{76}Li_2MgN_4Si_4$	$C_{21}H_{56}LiMgN_3Si_3$	$C_{58}H_{156}Li_2Mg_4N_6OSi_{10}$
M_r	364.3	469.1	337.0	619.5	466.2	1345.9
Cryst size (mm)	0.5 × 0.4 × 0.3	0.44 ×0.38 × 0.24	0.32 × 0.26 × 0.03	0.42 × 0.26 × 0.08	0.20 × 0.16 × 0.14	0.28 × 0.25 × 0.12
Cryst syst	Orthorhombic	Triclinic	Triclinic	Tetragonal	Monoclinic	Monoclinic
Space group	$P2_12_12_1$	$P\bar{1}$	$P\bar{1}$	$P4_32_12$	$P2_1/n$	$P2_1/c$
a (Å)	30.8877(9)	9.6476(5)	12.6467(7)	11.1275(7)	9.8686(3)	14.1664(5)
b (Å)	12.9370(2)	11.0862(6)	12.7597(7)		16.9877(7)	30.7009(9)
c (Å)	18.9561(3)	15.5535(6)	15.1259(8)	36.035(5)	19.5686(8)	21.7025(7)
α (deg)		104.171(4)	80.209(4)			
β (deg)		96.327(4)	69.849(5)		97.643(3)	95.679(3)
γ (deg)		111.437(5)	79.137(4)			
V (Å^3)	7574.7(3)	1464.12(12)	2235.7(2)	4461.9(7)	3251.4(2)	9392.6(5)
Z	12	2	4	4	4	4
μ (mm^{-1})	0.212	0.203	0.235	0.167	0.176	0.199
Trans coeff range	0.877–1.000	0.916–0.953	0.929–0.993	0.933–0.987	0.887–1.000	0.946–0.977
T (K)	123	150	150	150	123	150
Reflns measd	33974	9680	15192	9197	27494	64952
Unique reflns	14461	5839	9068	4486	9417	20427
R_{int}	0.0488	0.0181	0.0365	0.0648	0.0441	0.0437
Reflns with $F^2 > 2\sigma$	11908	4761	4852	1571	5767	11406
Refined params	664	323	415	199	269	877
R (on F, $F^2 > 2\sigma$)[a]	0.0845	0.0340	0.0355	0.0478	0.0469	0.0386
R_w (on F^2, all data)[a]	0.1763	0.0936	0.0643	0.0991	0.1178	0.0861
Goodness of fit S[a]	1.147	1.079	0.688	0.695	0.937	0.853
Max, min electron density (e Å^{-3})	0.56, –0.48	0.42, −0.34	0.23, −0.20	0.29, −0.23	0.48, −0.46	0.47, −0.25

[a]Conventional $R = \Sigma||F_o|-|F_c||/\Sigma|F_o|$; $R_w = [\Sigma w(F_o^2-F_c^2)^2/\Sigma w(F_o^2)^2]^{1/2}$; $S = [\Sigma w(F_o^2-F_c^2)^2/(\text{no. data - no. params})]^{1/2}$ for all data

[LiMgR$_3$] (1)

^{1}H NMR spectrum of **1** in C_6D_6 solution

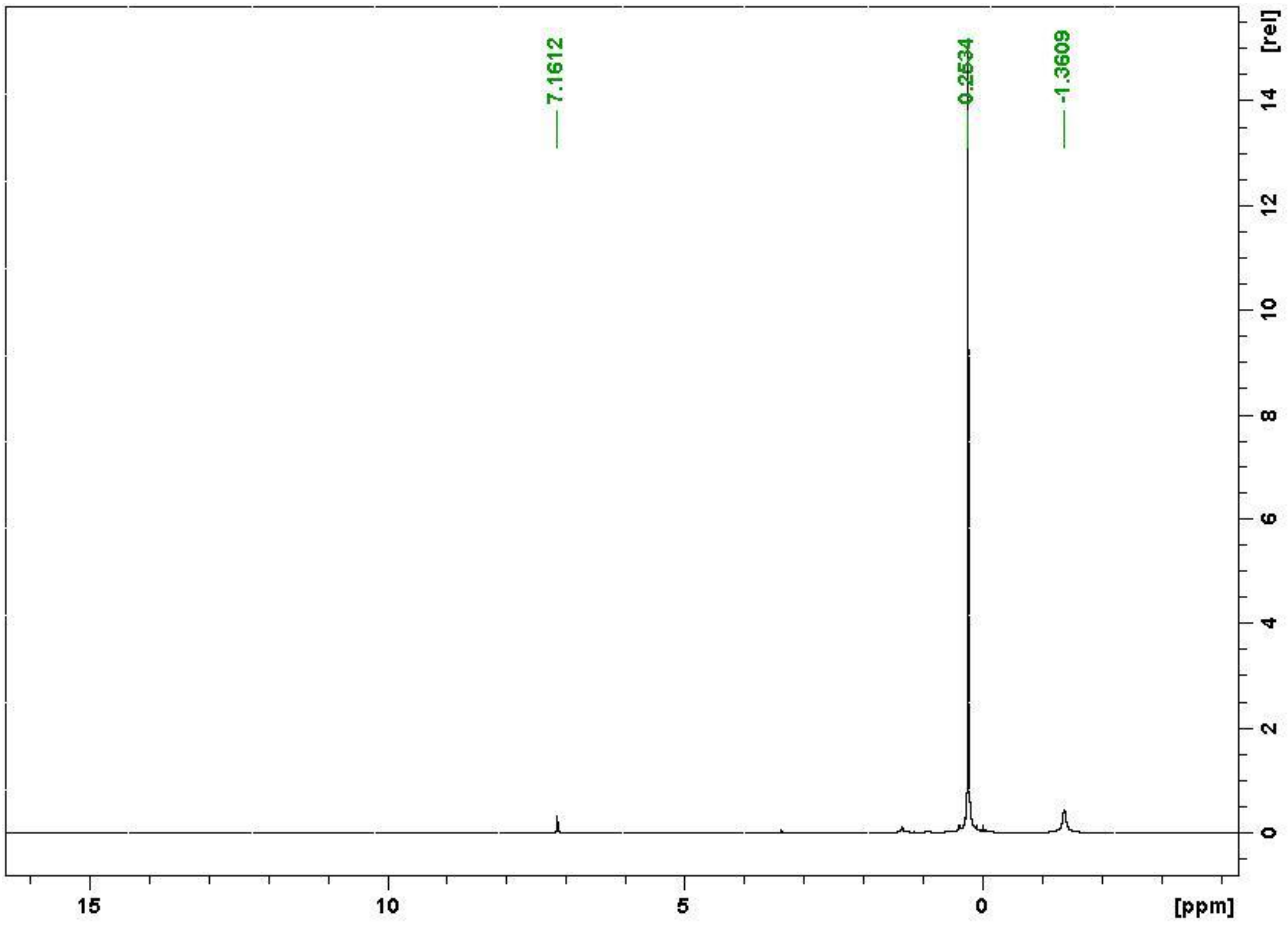

Figure S 1

$^{13}C\{^{1}H\}$ NMR spectrum of **1** in C_6D_6 solution

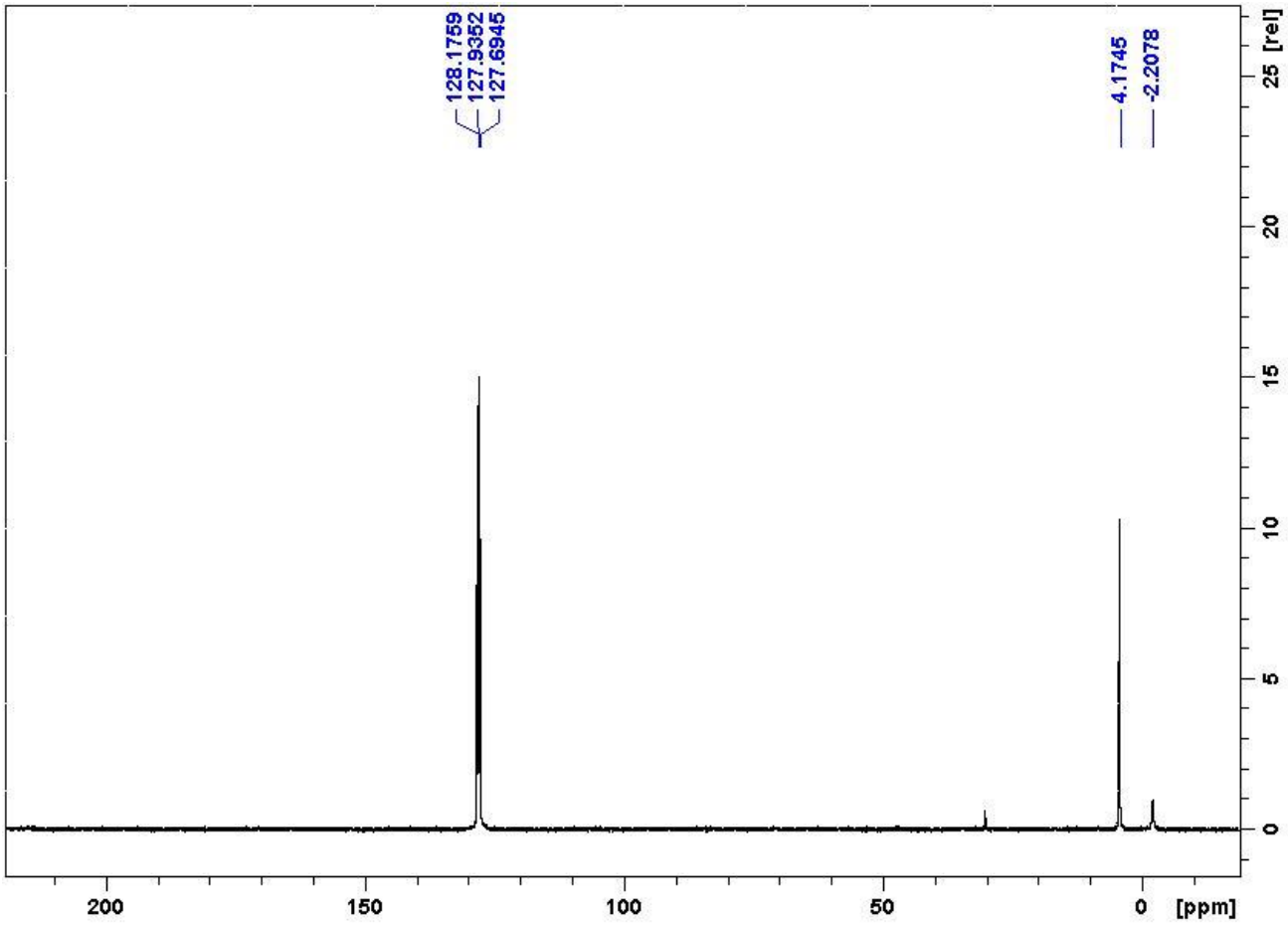

Figure S 2

^{7}Li NMR spectrum of **1** in C_6D_6 solution

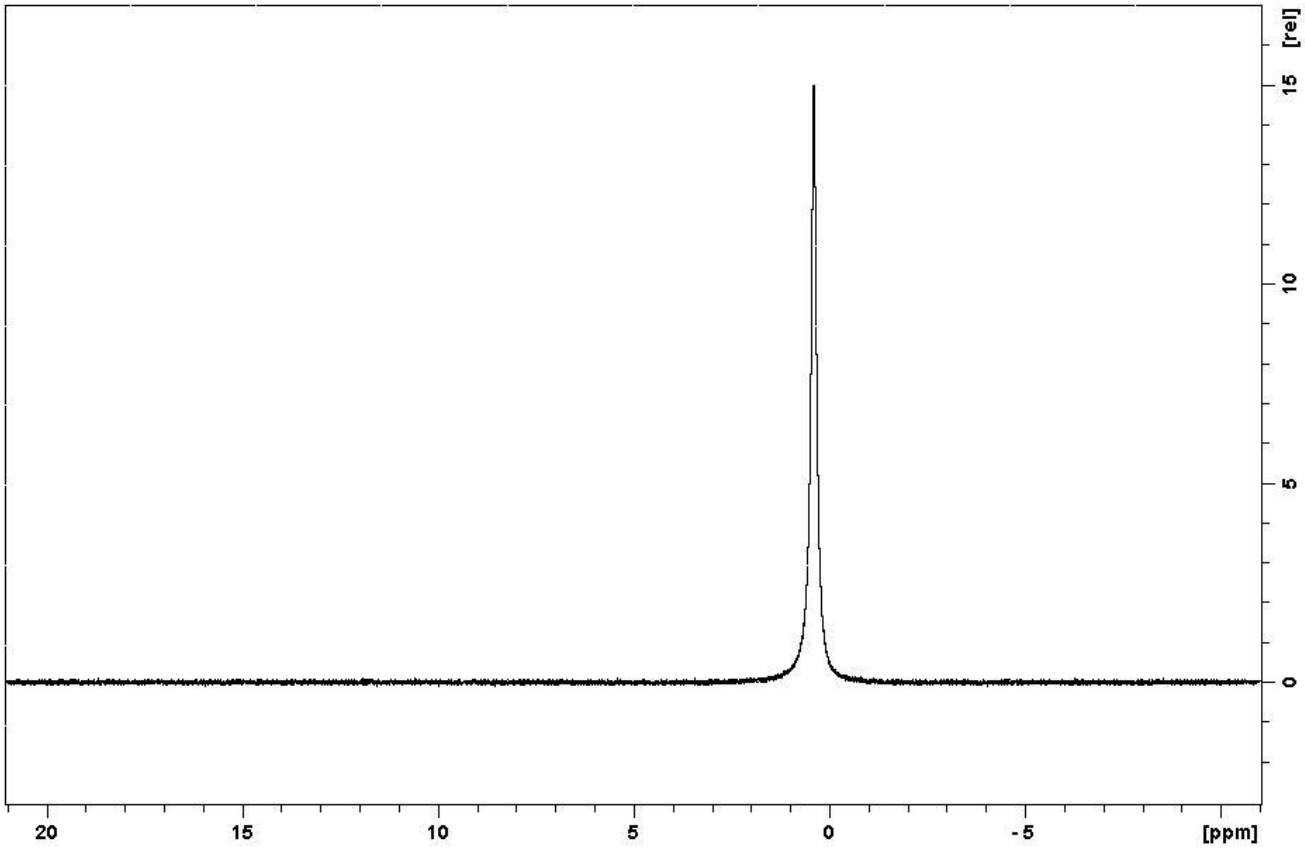

Figure S 3

[{(THF)LiMgR$_3$}$_\infty$] (2)

^{1}H NMR spectrum of **2** in C_6D_6 solution

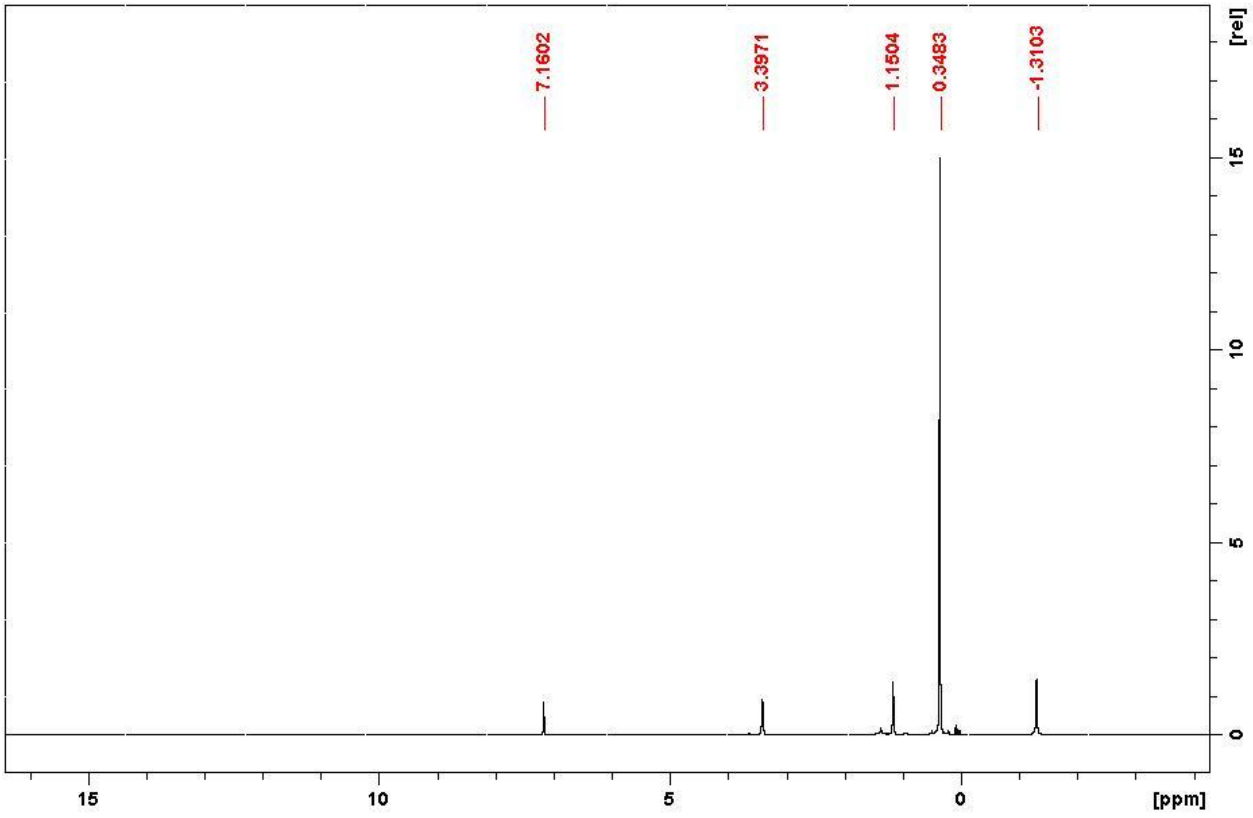

Figure S 4

$^{13}C\{^{1}H\}$ NMR spectrum of **2** in C_6D_6 solution

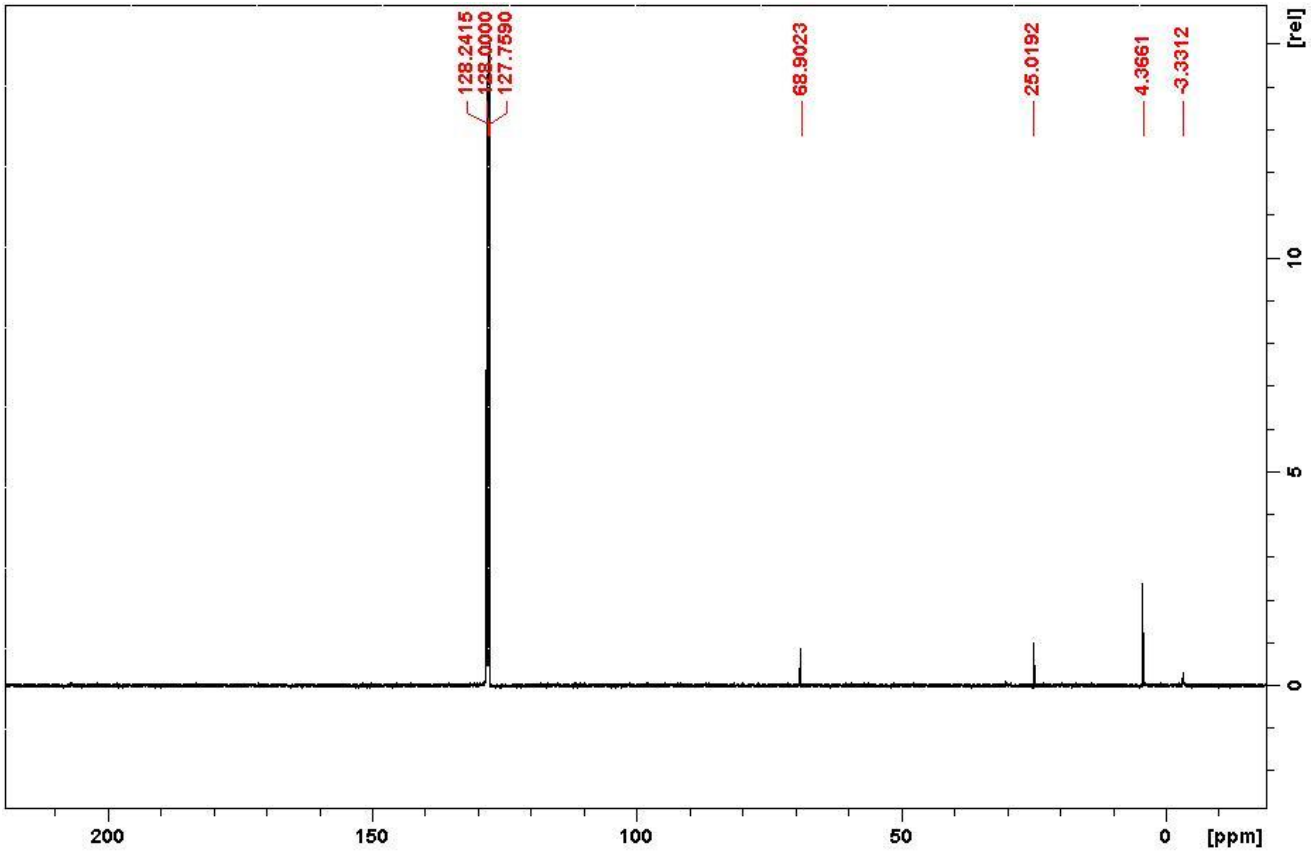

Figure S 5

^{7}Li NMR spectrum of **2** in C_6D_6 solution

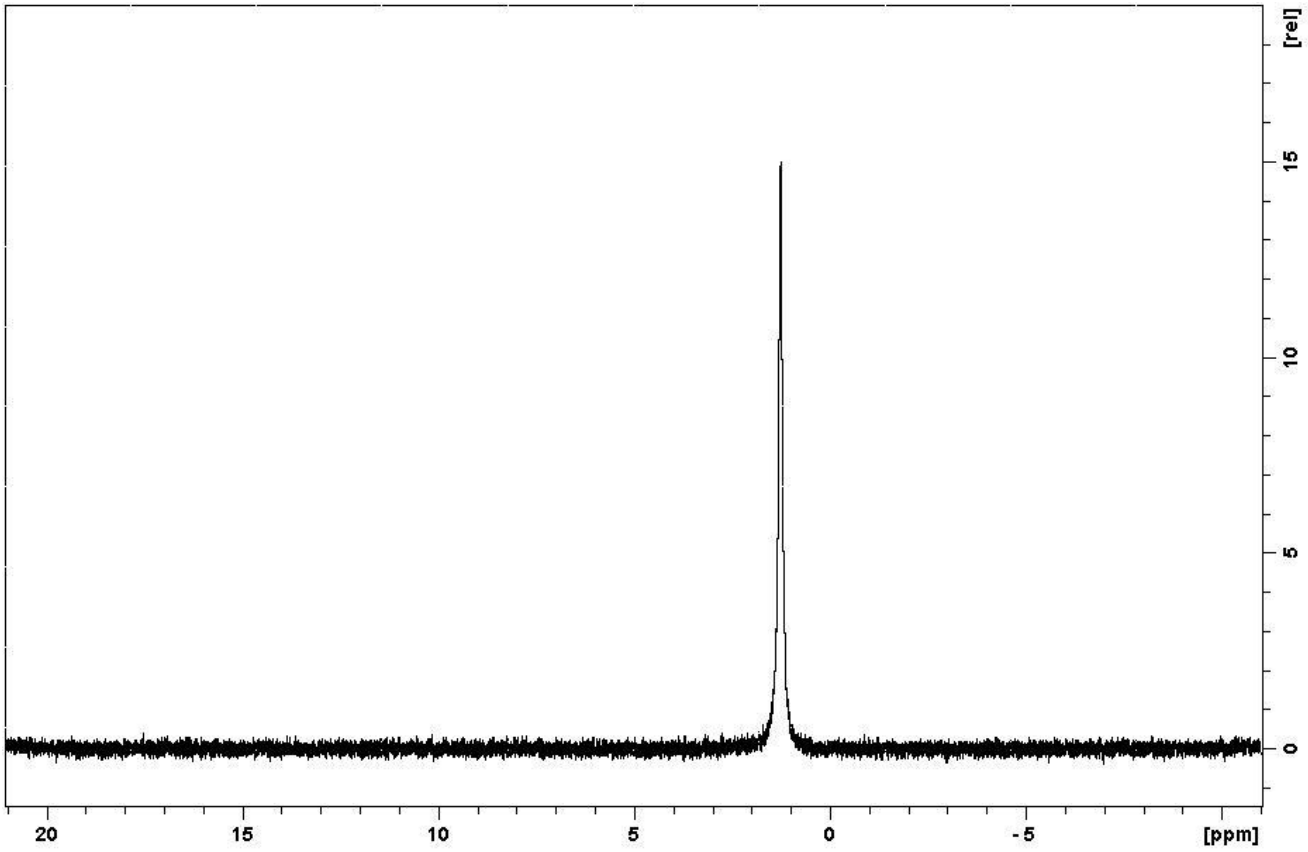

Figure S 6

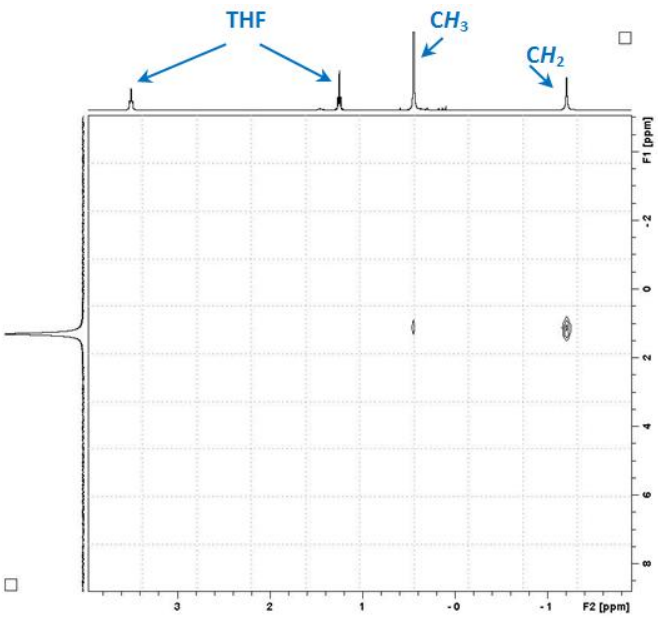

HOESY experiment showing cross-peaks between ^{1}H (x-axis) and ^{7}Li (y-axis) in **2**.

Figure S 7

[{(dioxane)$_2$LiMg(CH$_2$SiMe$_3$)$_3$}$_\infty$] (3)

^{1}H NMR spectrum of **3** in C_6D_6 solution

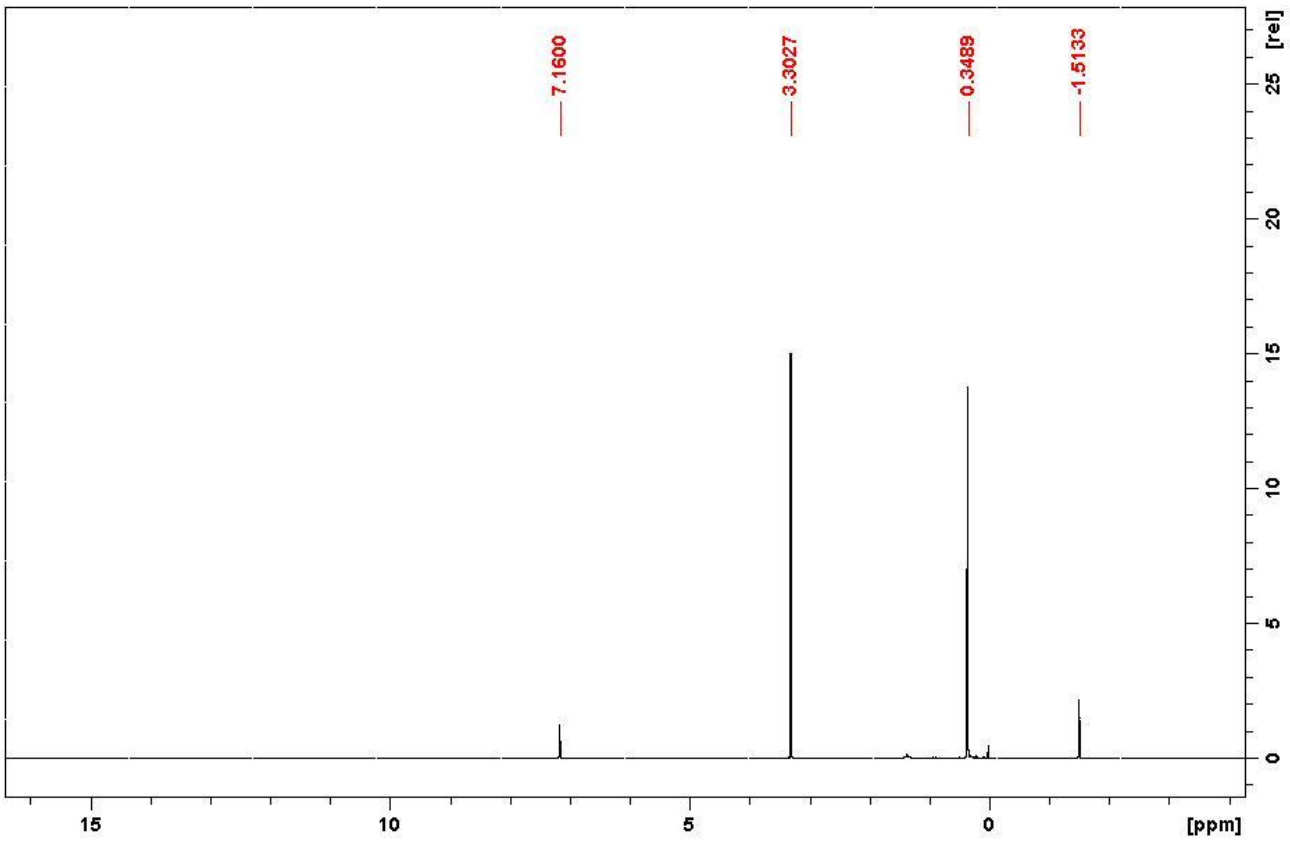

Figure S 8

^{7}Li NMR spectrum of **3** in C_6D_6 solution

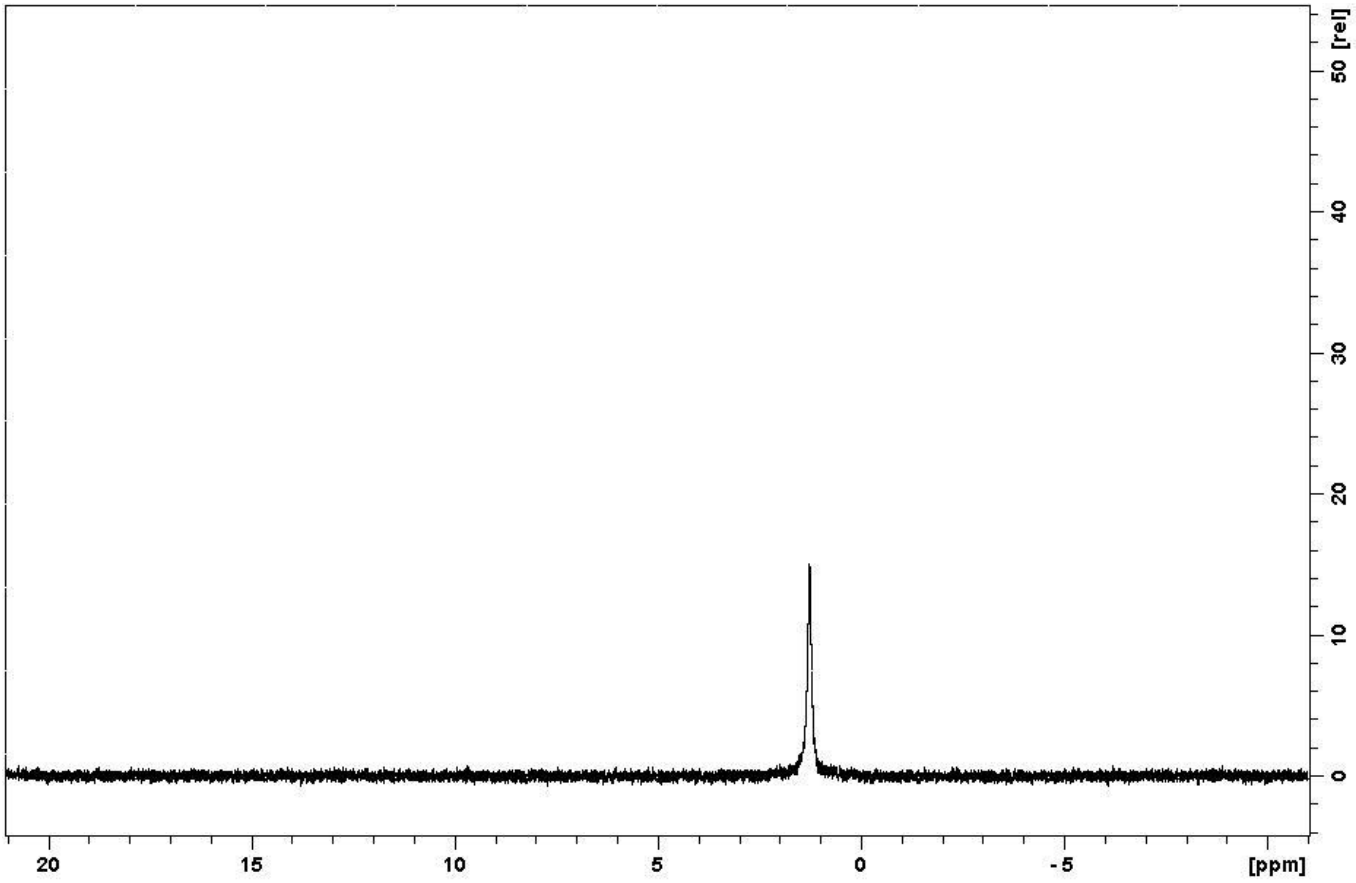

Figure S 9

Variable temperature experiment of **3** in deuterated toluene showing splitting of the M-CH_2 peak at 215 K from the two bridging and one terminal R group (S10a) and the broadening of the dioxane signal (S10b).

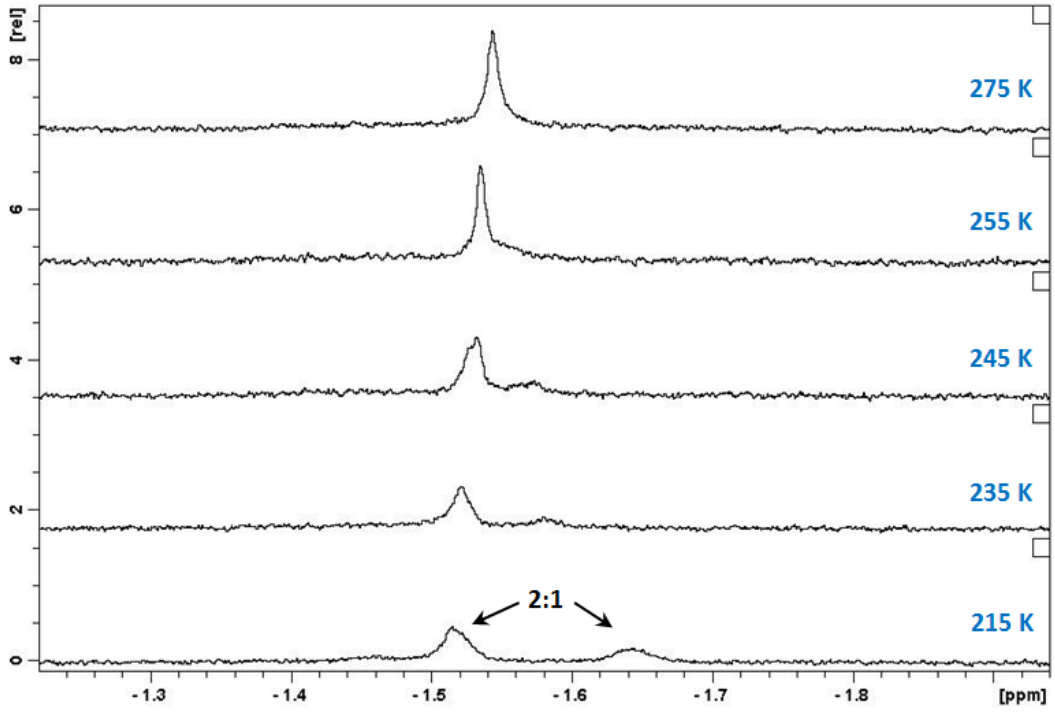

Figure S 10a

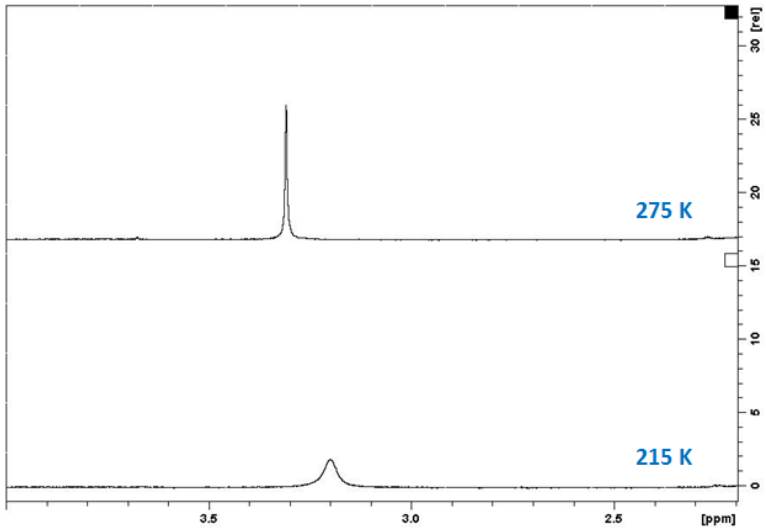

Figure S 10b

[{(dioxane)$Li_2Mg_2R_6$}$_\infty$] (4)

^{1}H NMR spectrum of **4** in C_6D_6 solution

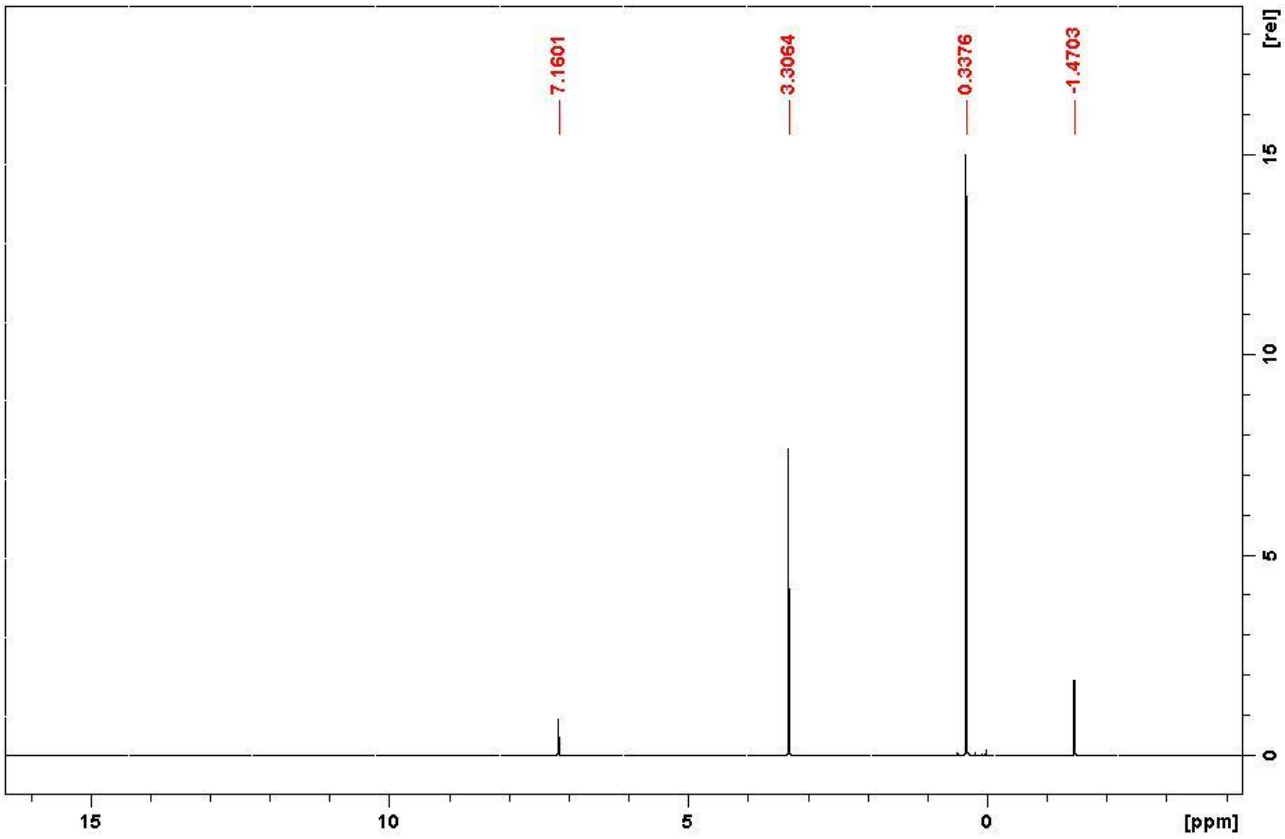

Figure S 11

Variable temperature experiment of **4** in deuterated toluene showing splitting of the M-CH_2 peak at 215 K from the inequivalent R groups.

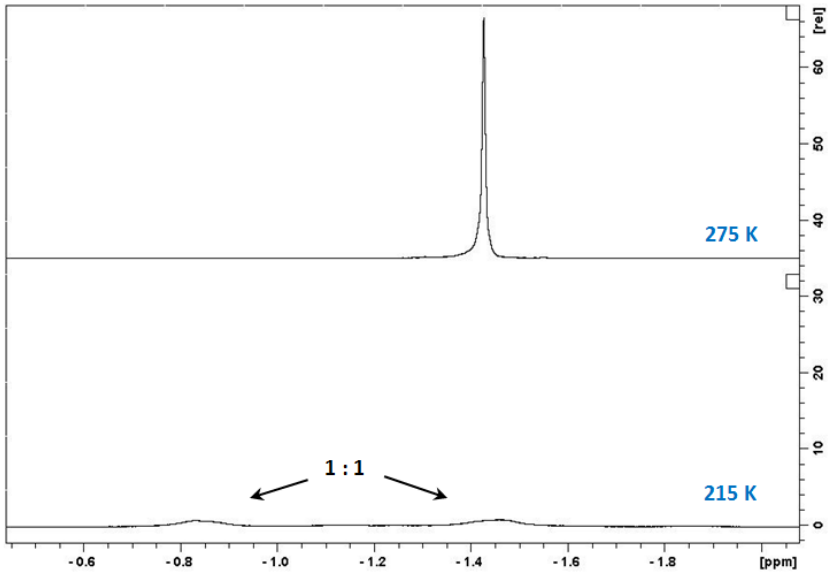

Figure S 12

[(TMEDA)$_2$Li$_2$MgR$_4$] (5)

^{1}H NMR spectrum of **4** in C_6D_6 solution

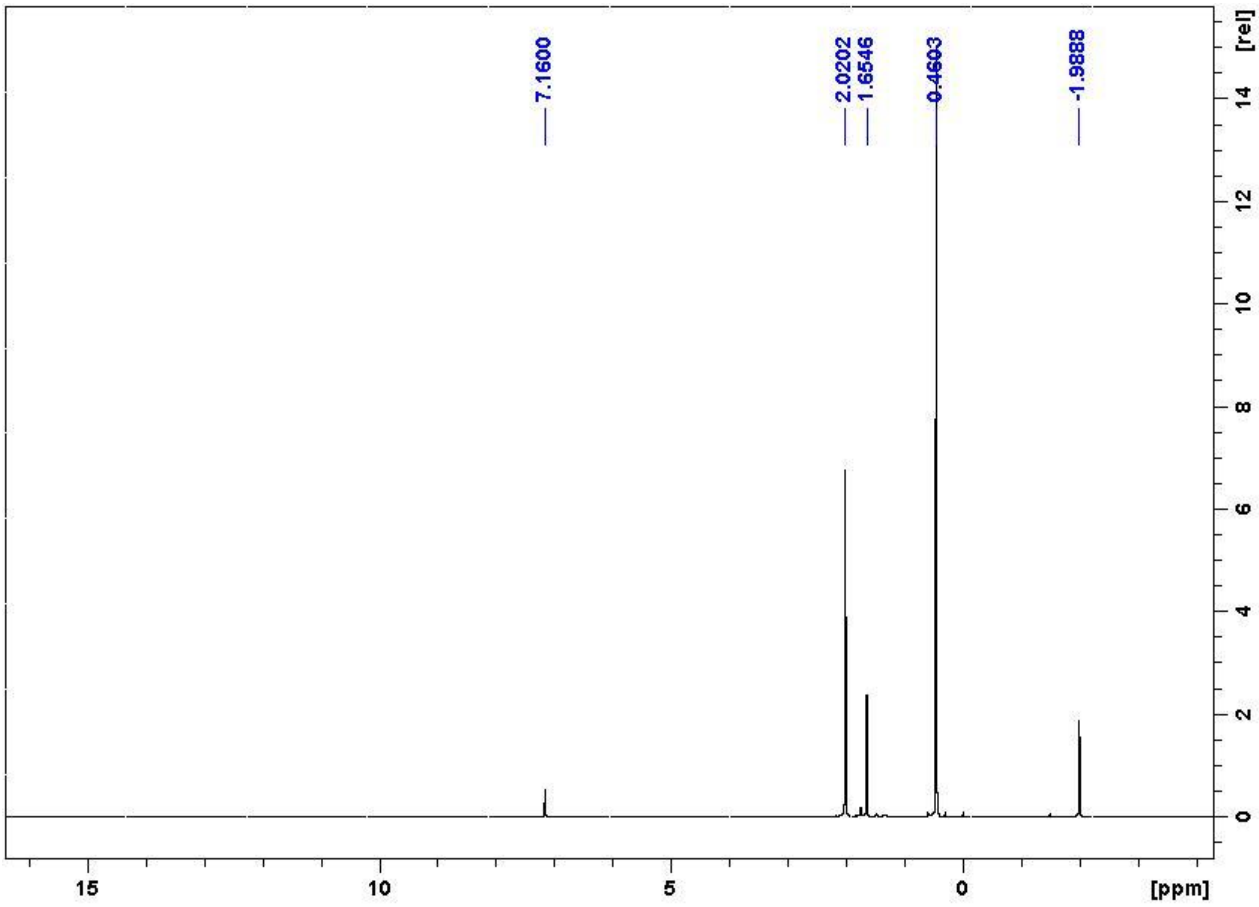

Figure S 13

$^{13}C\{^{1}H\}$ NMR spectrum of **5** in C_6D_6 solution

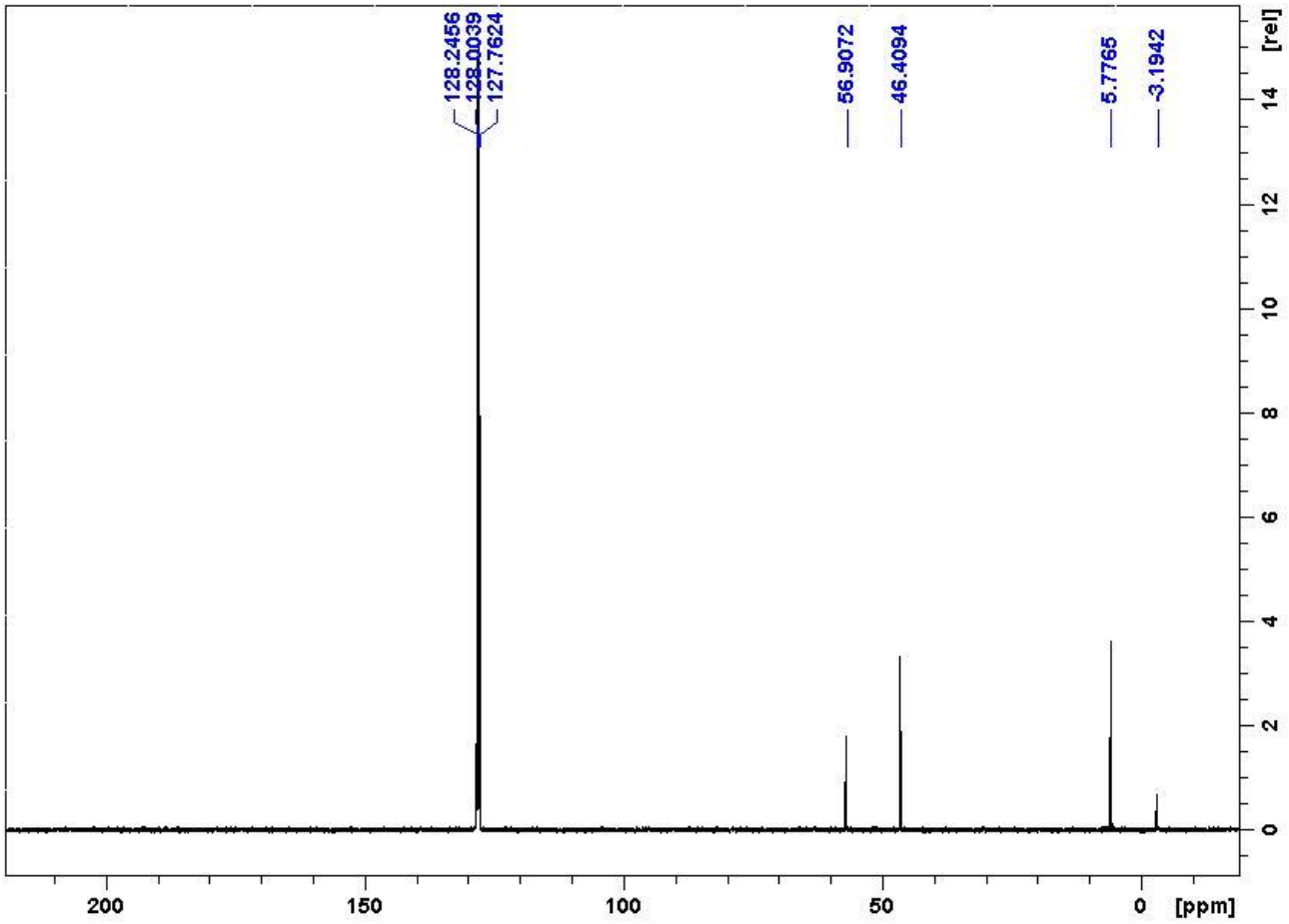

Figure S 14

^{7}Li NMR spectrum of **5** in C_6D_6 solution

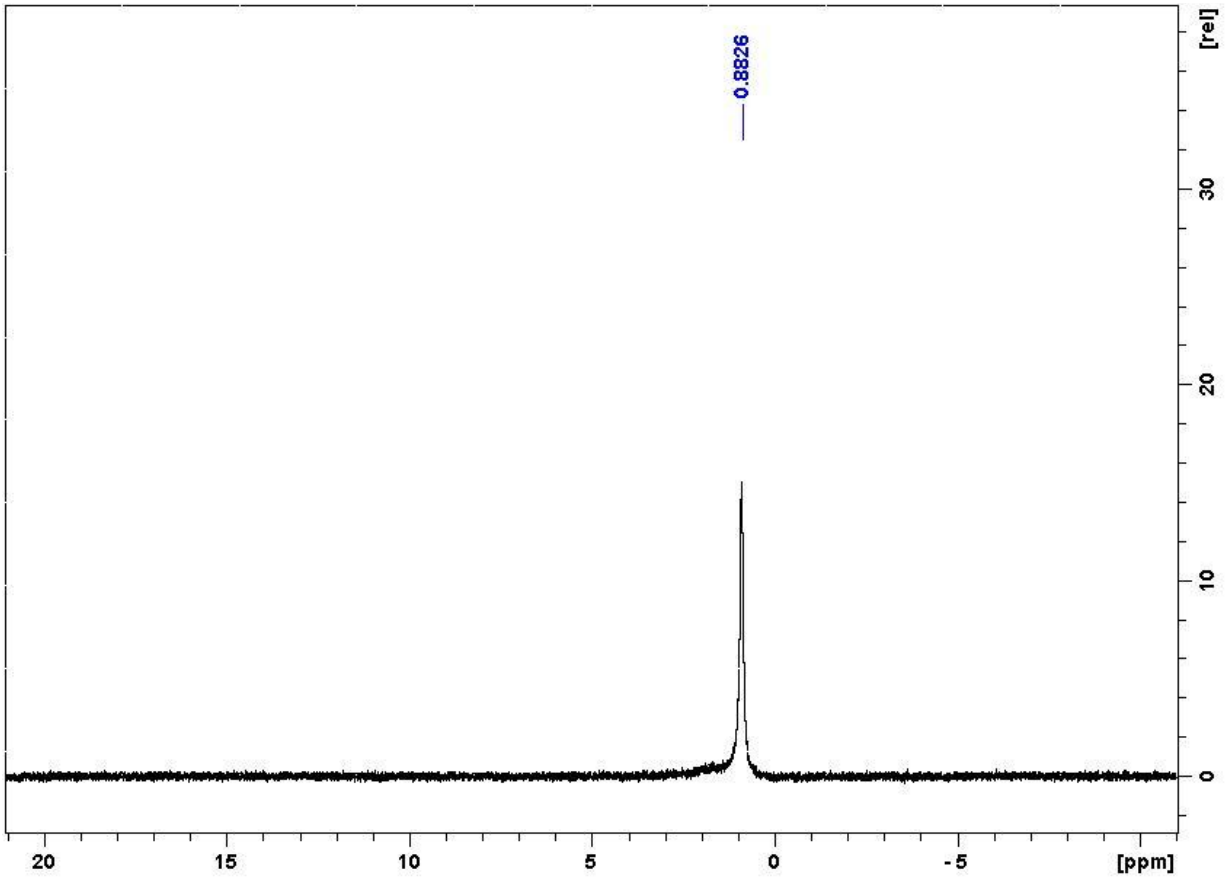

Figure S 15

[(PMDETA)LiMgR_3] (6)

^{1}H NMR spectrum of **6** in C_6D_6 solution

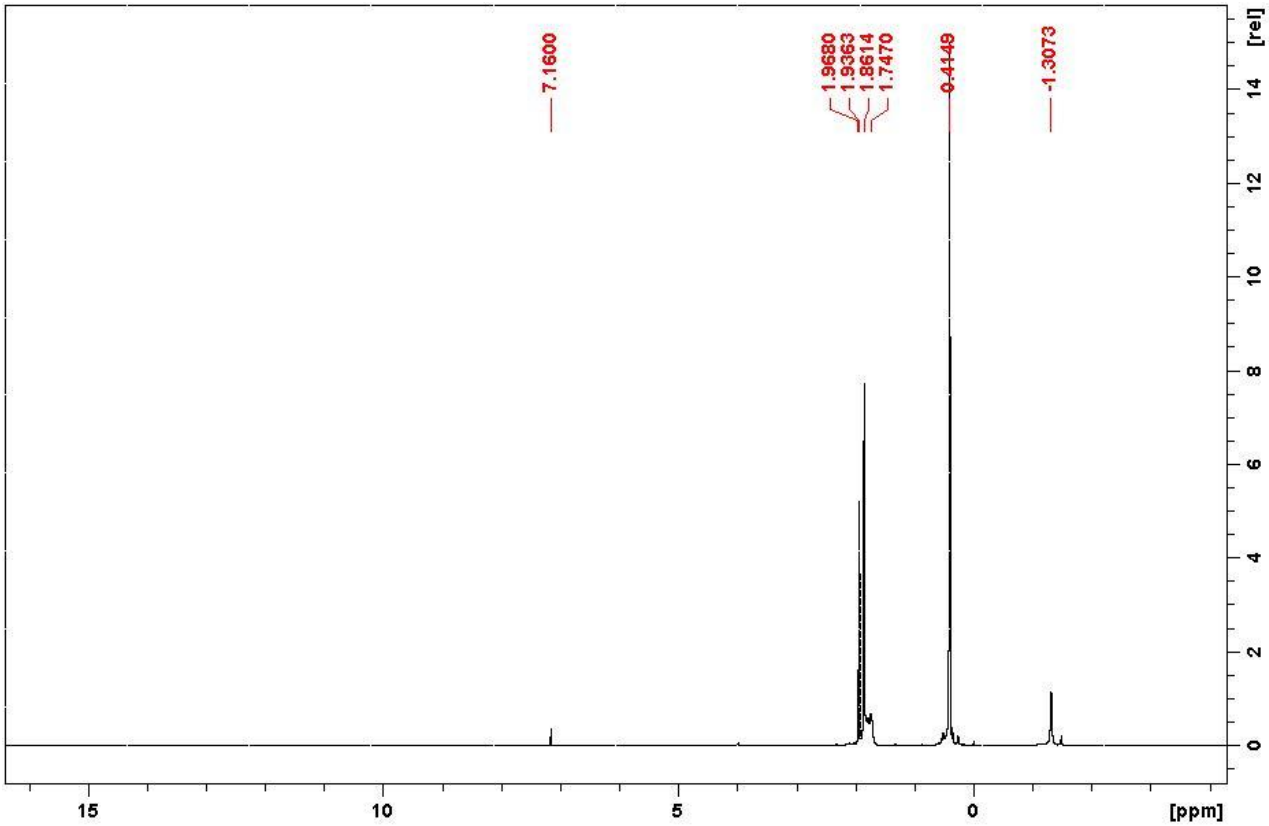

Figure S 16

$^{13}C\{^{1}H\}$ NMR spectrum of **6** in C_6D_6 solution

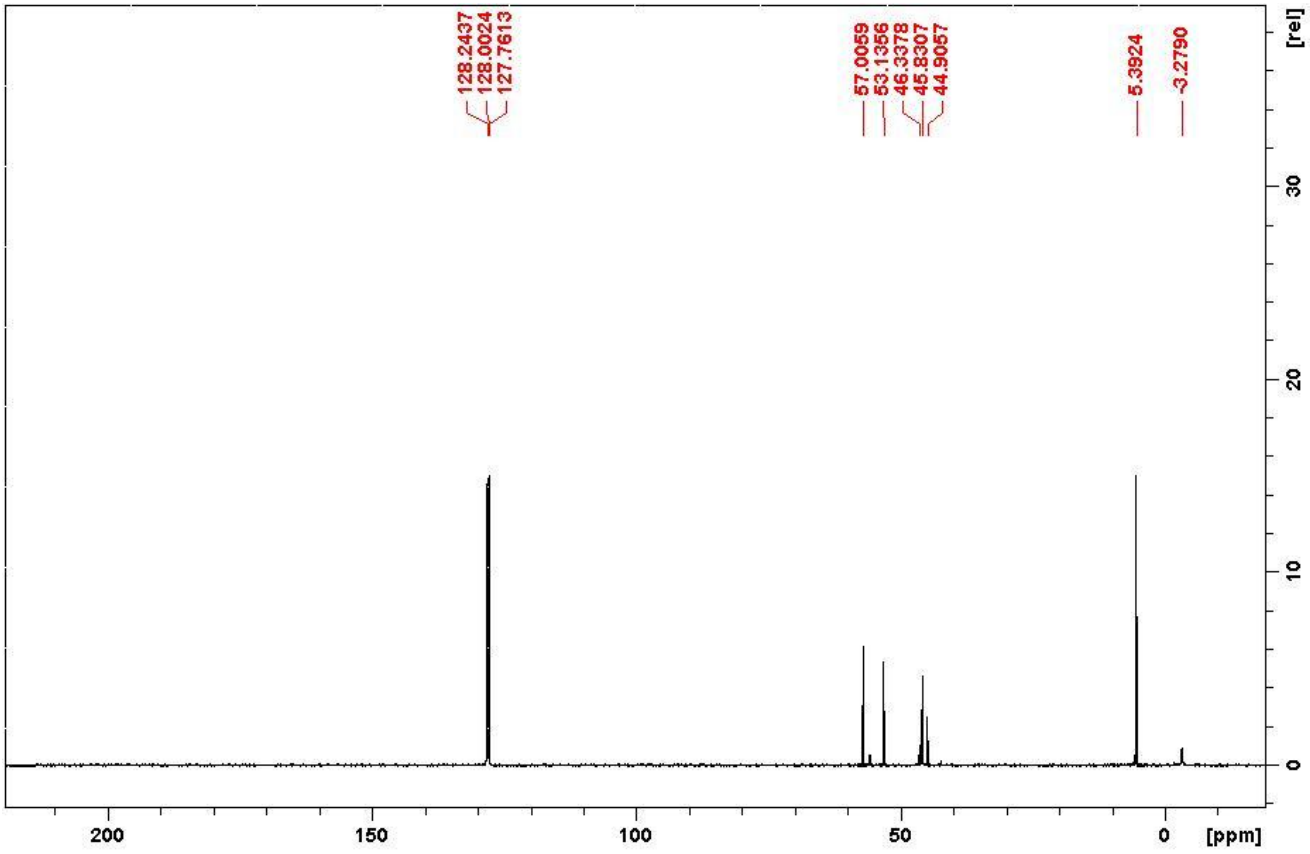

Figure S 17

^{7}Li NMR spectrum of **6** in C_6D_6 solution

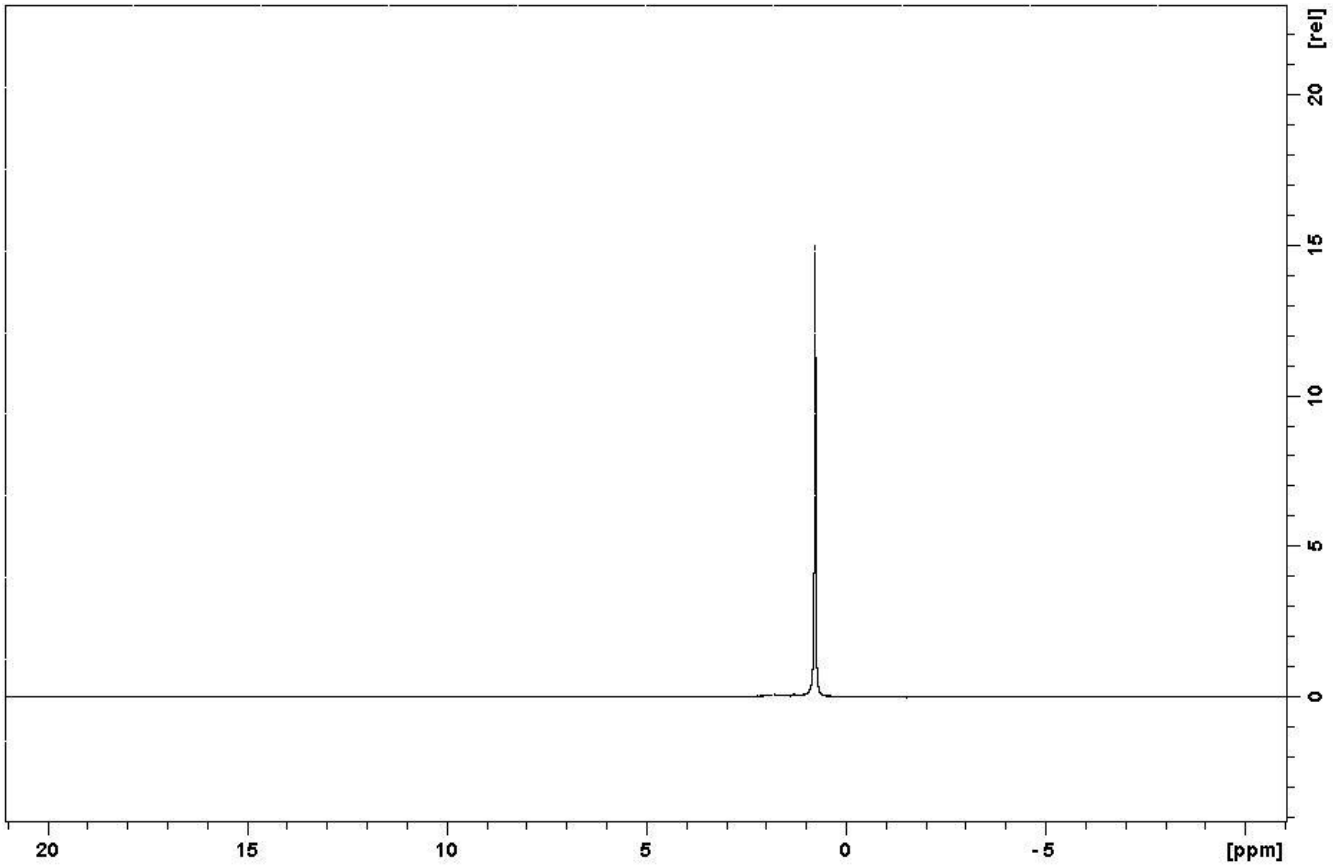

Figure S 18

[{(PMDETA)$_2$Li$_2$MgR$_3$}$^+${Mg$_3$R$_6$(OR)}$^-$] (7)

^{1}H NMR spectrum of **7** in C_6D_6 solution

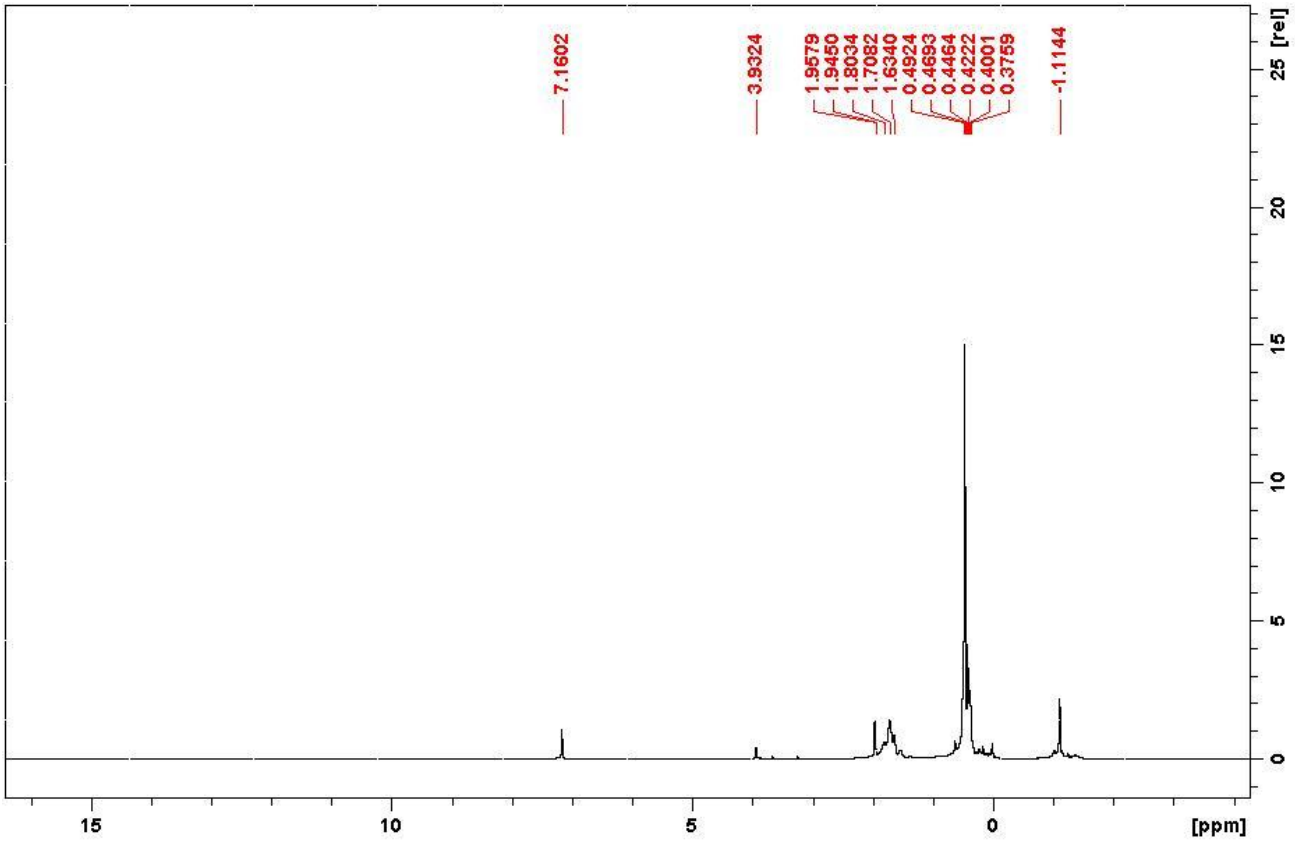

Figure S 19

^{7}Li NMR spectrum of **7** in C_6D_6 solution

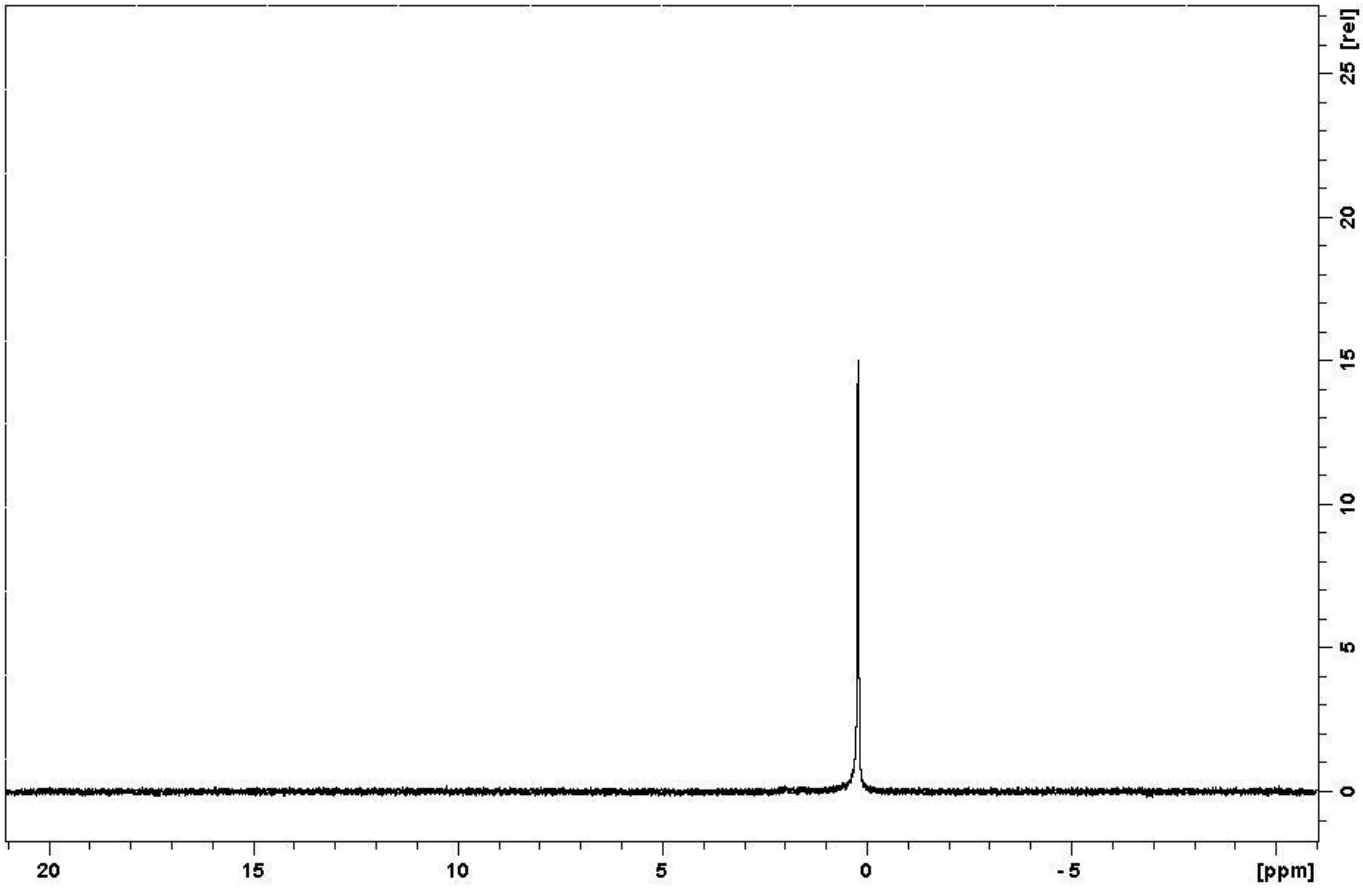

Figure S 20

DOSY Experiments

^{1}H NMR spectrum of [LiMg(CH_2SiMe_3)$_3$(THF)] (**2**), TPhN, PhN and TMS at 27 °C in C_6D_6 (traces of grease are also observed).

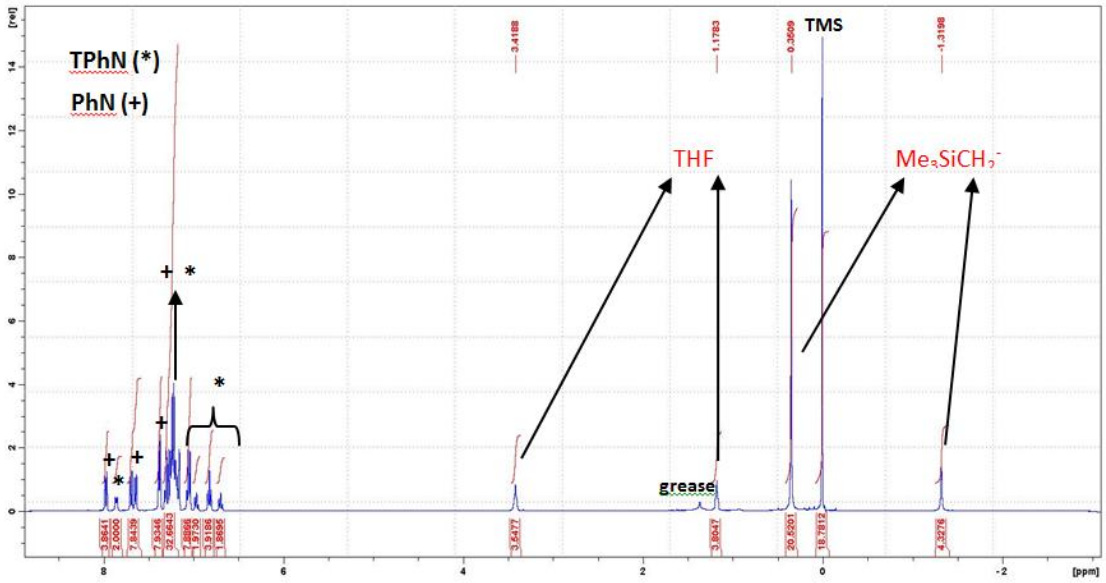

Figure S 21

^{1}H-DOSY NMR spectrum of **2**, and standards TPhN, PhN and TMS in C_6D_6 at 298 K (some traces of grease also observed)

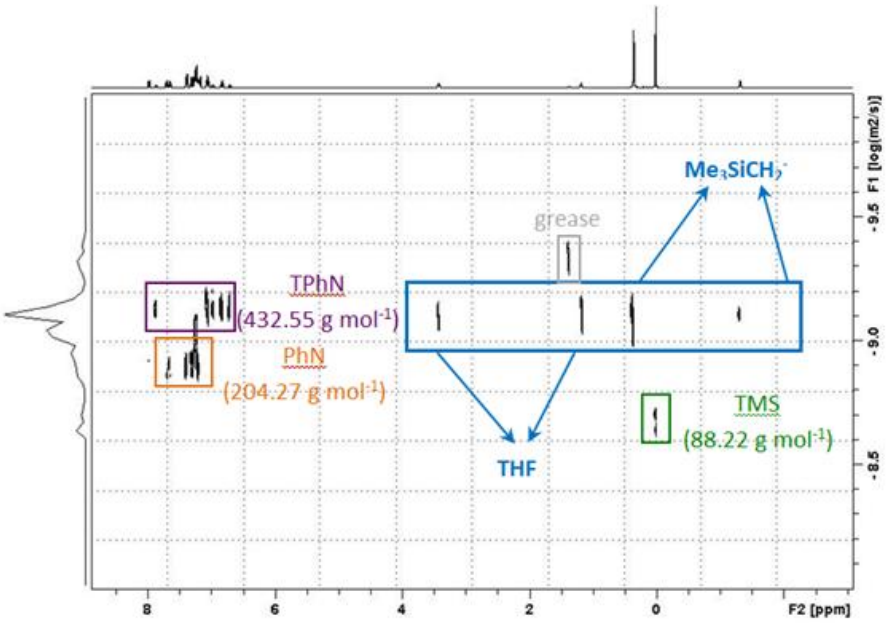

Figure S 22

log *D* – log FW representation from the ^{1}H-DOSY data obtained for the mixture of **2**, TPhN, PhN and TMS in C_6D_6 (data for the components of **2** is not included).

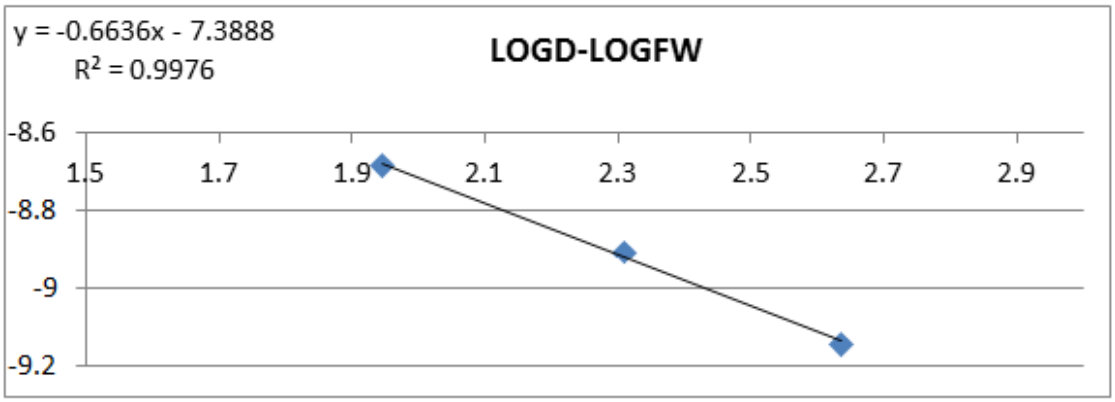

Figure S 23

Possible species of $LiMg(CH_2SiMe_3)_3(THF)]$ (**2**) in C_6D_6 with errors (in brackets) respect to the FW value predicted through the DOSY study.

FW predicted for Me_3SiCH_2-/THF in C_6D_6 = 410.37 (g mol-1)

A **$[LiMg(CH_2SiMe_3)_3(THF)]_3$**

$C_{48}H_{123}Mg_3Li_3O_3Si_9$ 1095.00 g mol^{-1} (63 %)

B **$[LiMg(CH_2SiMe_3)_3(THF)]_2$**

$C_{32}H_{82}Mg_2Li_2O_2Si_6$ 730.00 g mol^{-1} (44 %)

C **$[LiMg(CH_2SiMe_3)_3(THF)] \cdot C_6D_6$**

$C_{22}H_{41}D_6MgLiOSi_3$ 449.15 g mol^{-1} (9 %)

D **$[LiMg(CH_2SiMe_3)_3(THF)]$**

$C_{16}H_{41}MgLiOSi_3$ 364.00 g mol-1 (- 13 %)

Figure S 24

^{1}H-DOSY NMR spectrum of [(dioxane)$_2$LiMg(CH$_2$SiMe$_3$)$_3$] (**3**), TPhN, PhN and TMS at 27 °C in C_6D_6 (signal intensity of the MC*H*$_2$ cross point was increased for presentational purposes).

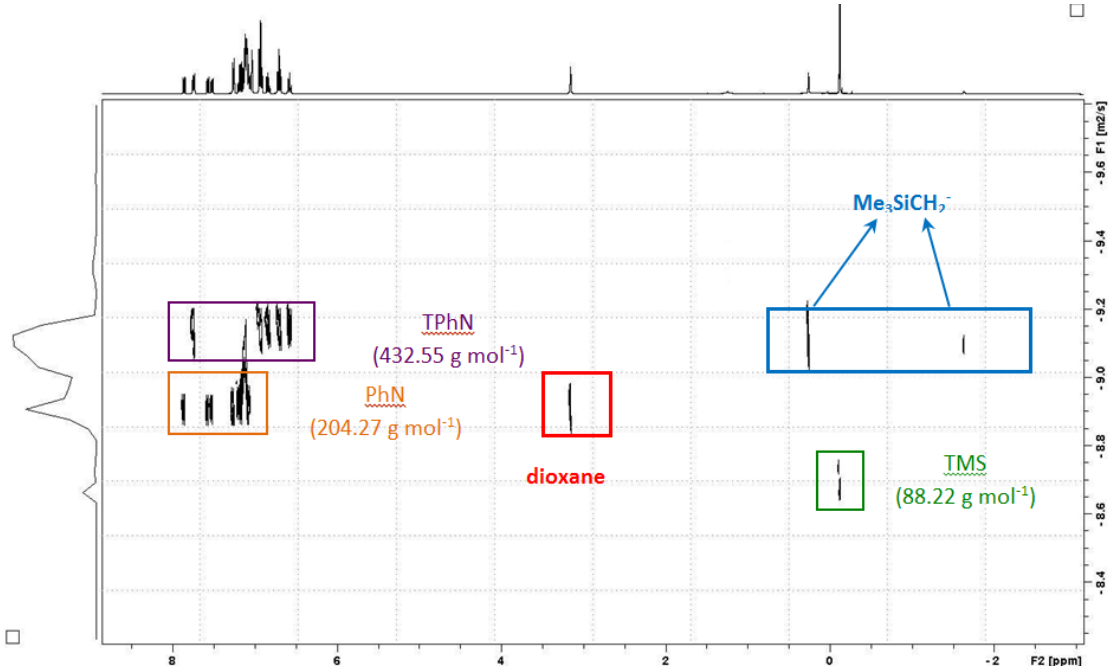

Figure S 25

log *D* – log FW representation from the ^{1}H-DOSY data obtained for the mixture of **3,** TPhN, PhN and TMS in C_6D_6 (data for the components of **3** is not included).

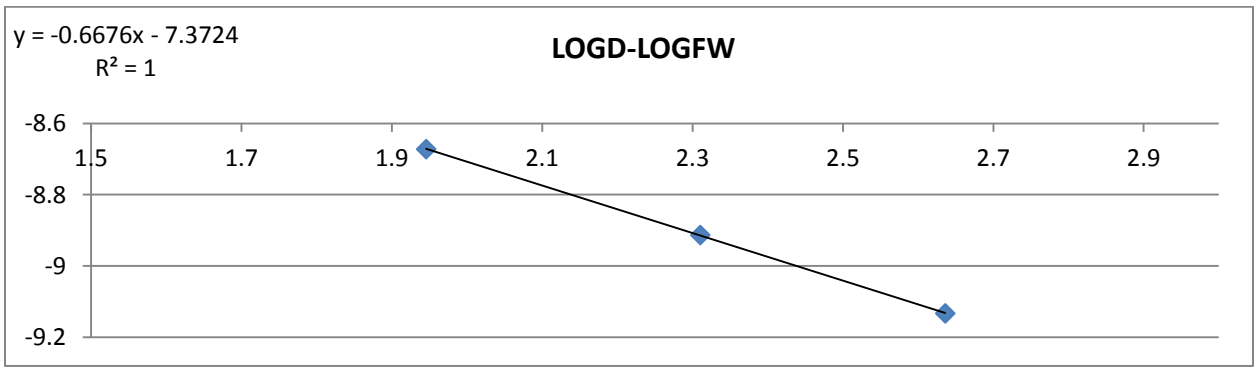

Figure S 26

^{1}H-DOSY NMR spectrum of [(dioxane)$Li_2Mg_2(CH_2SiMe_3)_6$] (**4**), TPhN, PhN and TMS at 27 °C in C_6D_6.

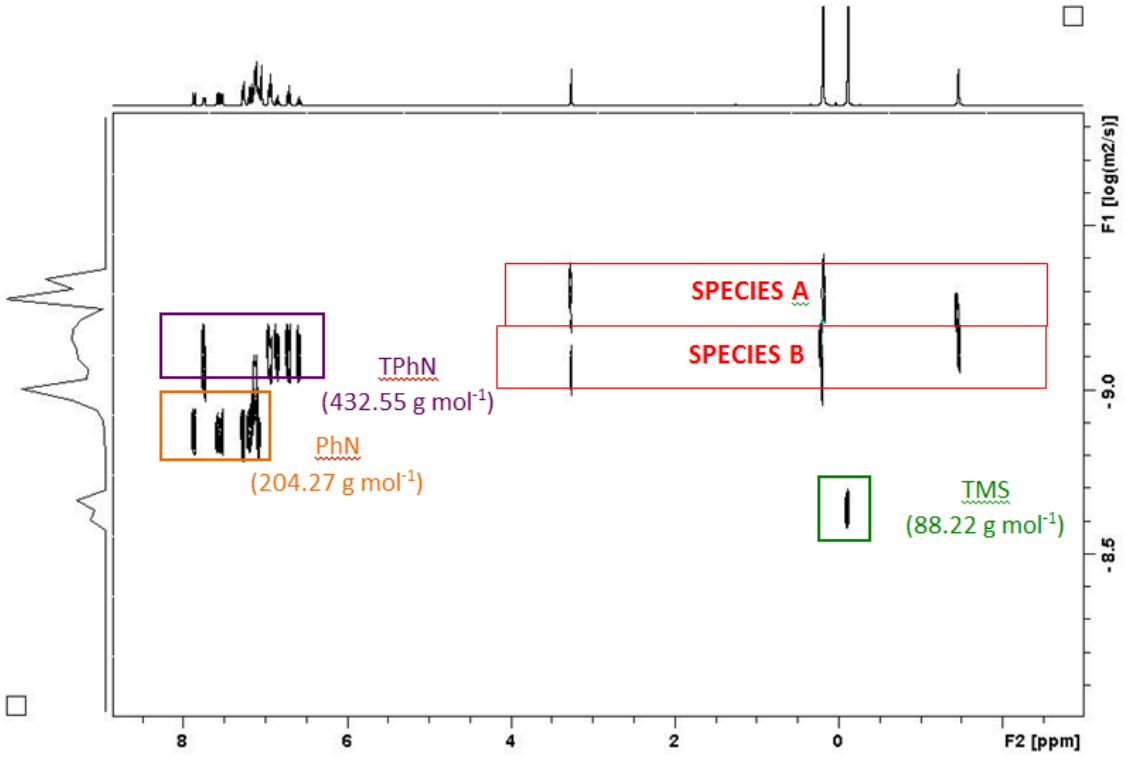

Figure S 27

^{1}H NMR spectrum of **4** in d_8-toluene solution at 298 K

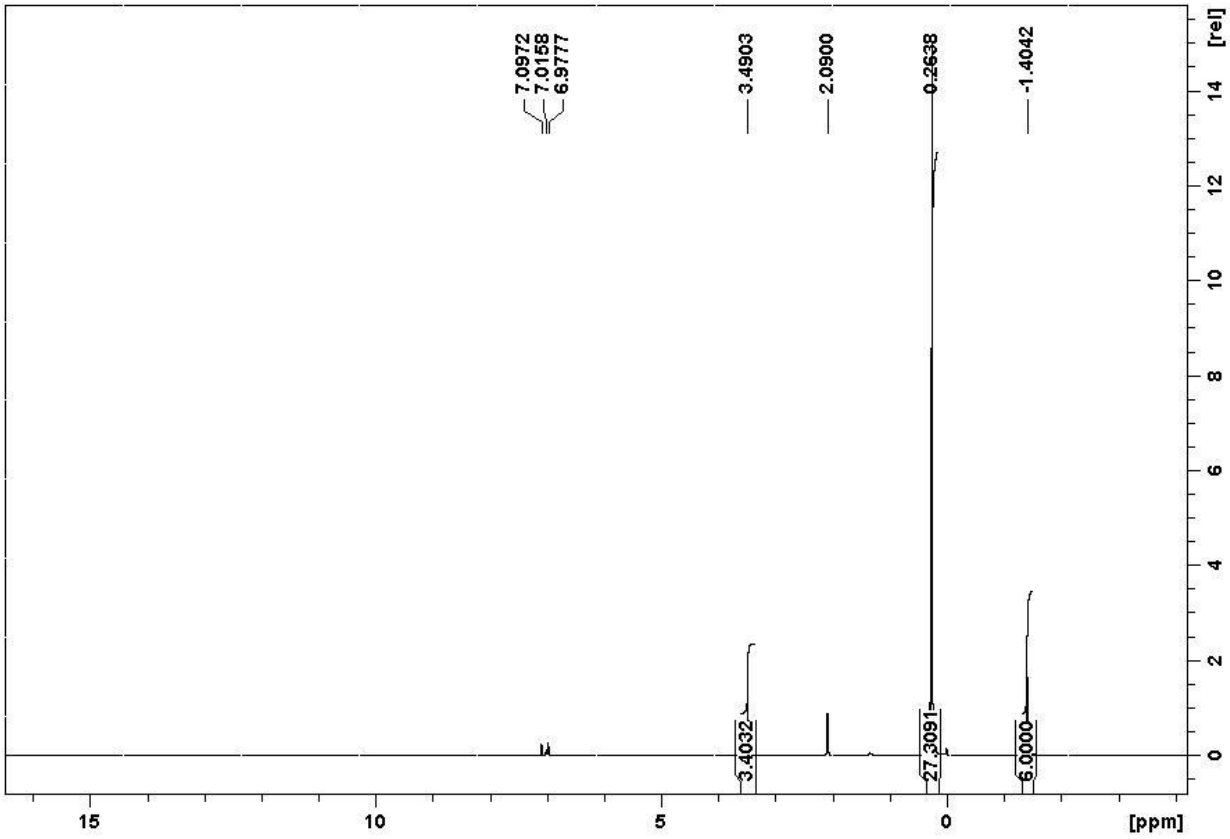

Figure S 28

^{1}H NMR spectrum of **4** in d_8-toluene solution at 270 K

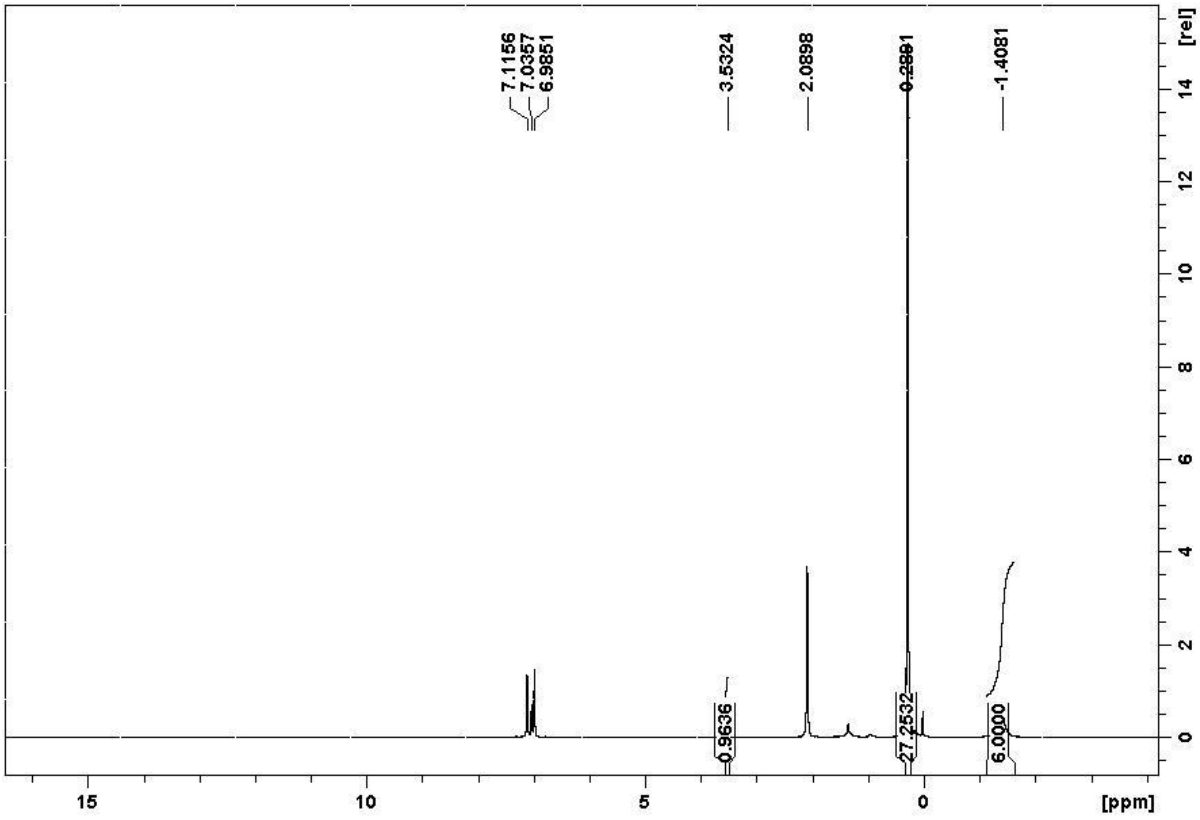

Figure S 29

^{1}H-DOSY NMR spectrum of dioxane, TPhN, PhN and TMS at 27 °C in C_6D_6 and log *D* – log FW representation from the ^{1}H-DOSY data obtained for the mixture of TPhN, PhN and TMS in C_6D_6.

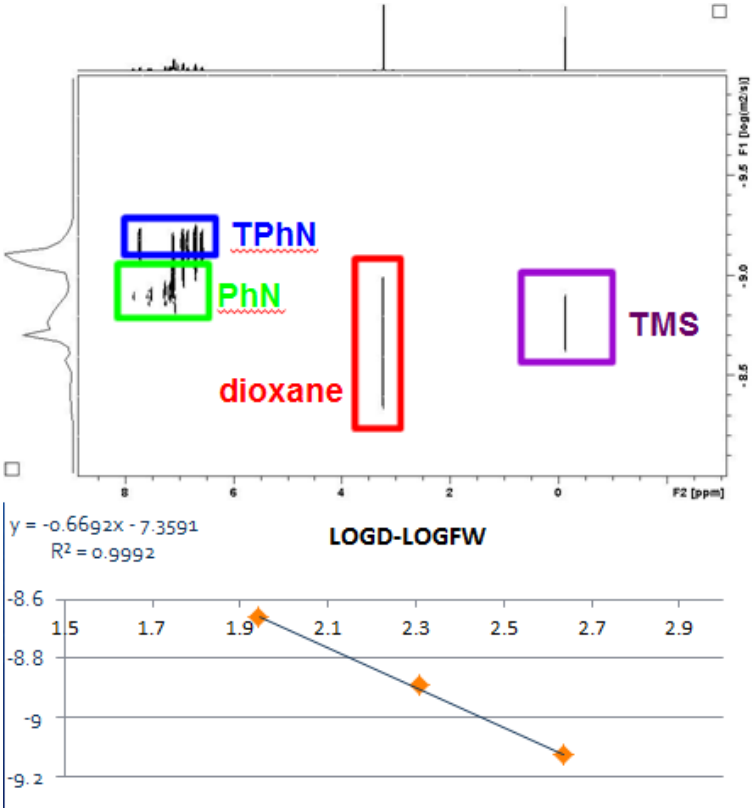

Figure S 30